Results in Chemistry 4 (2022) 100663

Contents lists available at ScienceDirect

Results in Chemistry

journal homepage: www.sciencedirect.com/journal/results-in-chemistry

Xanthomonadin mediated synthesis of biocidal and photo-protective silver nanoparticles (XP-AgNPs)

Narendra S. Salunkhe [a], Sunil H. Koli [a], Bhavana V. Mohite [b], Vikas S. Patil [c], Satish V. Patil [a,*]

[a] School of Life Sciences, Kavayitri Bahinabai Chaudhari North Maharashtra University, Jalgaon 425001, Maharashtra, India
[b] Department of Microbiology, Bajaj College of Science, Wardha 442001, Maharashtra India
[c] UICT, Kavayitri Bahinabai Chaudhari North Maharashtra University, Jalgaon 425001, Maharashtra, India

ARTICLE INFO

Keywords:
Xanthomonas sp.
Xanthomonadin
Pigments
Silver nanoparticles
SPF
Biocidal
Andtioxidant

ABSTRACT

Nanoparticles have drawn significant attention in recent years, owing to their unique electrical, optical, biocidal, and catalytic properties. The present study reports an environment friendly, green approach for silver nanoparticles (AgNPs) synthesis using bacterial yellow color pigment, xanthomonadin (XP) derived from *Xanthomonas* sp. After exposing the reaction mixture to sunlight, a visible colour shift and spectrophotometric measurement proved that nanosized silver particles (XP-AgNPs) were being synthesized by xanthomonadin. The size of XP–AgNPs was in the range between 30 and 100 nm, with the spherical shaped particles. The XP–AgNPs showed excellent biocidal activity against representative Gram positive and Gram negative organisms i.e. *Staphylococcus aureus*, *B. subtilis* and *Pseudomonas aeruginosa*, *Escherichia coli*. In addition, using standard assays, the photo-protecting/SPF enhancement of commercial sunscreens and DPPH radical scavenging activity of XP, and XP-AgNPs were evaluated. As a result, adding 4 % w/w xanthomonadin in commercial sunscreens have original SPFs 4 and 10 increases by 271 % and 85.2 %, respectively. XP and XP-AgNPs showed significant antioxidant activities with the IC_{50} values of 46.21 μg/mL and 21.62 μg/mL, respectively. In conclusion, xanthomonadin mediated silver nanomaterial with photo protecting, antioxidant and biocidal potential has been reported.

Introduction

In recent years, the nano sized particles of various metals have drawn significant attention owing to their unique properties over the bulk of metals. The characteristics, small size, shape, and structural distribution of metal particles improve the optical, electrical, and catalytic properties [1]. Therefore, nano sized metal particles are utilized mainly in electronics, medicine, and agriculture. As a result, around 3,862 nano based products are available within the market, with an estimated annual nanomaterial production rate of up to thousands of tons/year [2,3]. Still, the demand for nanomaterials continuously increases year and year basis.

Several methods were successfully used to produce nano-materials to meet market demand; chemical and physical methods. However, these are considered non eco friendly and potentially hazardous due to utilizing the toxic chemicals and high energy to reduce bulk metal into nano-formed. Besides, several carcinogenic and non-biodegradable chemicals use in a chemical method as reducing and stabilizing agents, which raise potential human and environmental concerns [4,5]. Due to the limitations of chemical and physical methods, in recent times, researchers have been focused on green approaches to develop simple, eco-friendly, non-hazardous procedures consisting of non-toxic chemicals as reducing and stabilizing agents [6].

Among the various nano sized metal particles, silver and gold nanoparticles have gained wide attention in both research and industrial platform due to their applications in diverse areas such as textiles, food packaging, biosensors, nano composites, nano electronics, nano diagnostics, cosmetics, bioremediation, and a biocidal agent [3,7,8]. The nano sized silver particles are preferred as an antimicrobial agent in biomedical use owing to their high biocidal potential against multi-drug resistant bacterial pathogens (Table 1).

The nano sized silver particles are also utilized in sunscreen preparations to enhance sun protection and provide better and longer protection against sunburn [17,18]. Besides these green synthesized nano silver was reported as good nano catalyst for oxygen evolving reactions and reduction of organic dye pollutant, as electrochemical sensor and

* Corresponding author at: School of Life Sciences, North Maharashtra University, Post Box - 80, Jalgaon 425001, Maharashtra, India.
E-mail addresses: svpatil@nmu.ac.in, satish.patil7@gmail.com (S.V. Patil).

https://doi.org/10.1016/j.rechem.2022.100663
Received 5 September 2022; Accepted 13 November 2022
Available online 15 November 2022
2211-7156/© 2022 The Authors. Published by Elsevier B.V. This is an open access article under the CC BY-NC-ND license (http://creativecommons.org/licenses/by-nc-nd/4.0/).

for its antibacterial potential [19–22]. The purpose behind 'green' nanomaterial synthesis is to make the process easy i.e. one-step and ecofriendly, hence use of reducing natural green materials like enzymes, ascorbic acid, flavonoids, phenolics, and pigments and capping agents like natural polymers i.e. protein, and starch of plant, bacteria, and algae [3,7,8]. Several international regulatory agencies have also suggested a "safe by design" approach to minimize the harmful effects of nanomaterial and promote their sustainable use in different applications [3,23].

Among the microbial pigments, bacterial pigments have a unique feature of protecting the bacteria from oxidative stress and UV radiation and are also involved in quorum sensing. The bacterial strain Xanthomonas sp. is a Gram negative rod shape bacterium, generally studied for its pathogenesis in plants. However, on the other hand, several strains of Xanthomonas are important as producers of the exopolysaccharide xanthan, utilized in the food and pharmaceutical industries. In addition, the Xanthomonas sp. produce yellow membrane bound pigments called xanthomonadin (XP), a structurally distinct class of halogenated, arylpolyene, water insoluble pigments. Similar to carotenoid pigments, XP structure also consists of the long polyene moiety. Carotenoids' polyene moiety has been speculated to be required for photoprotective action [24]. These aforementioned properties of XP grabbed researchers' attention, owing to its unique properties such as pigments that protect the bacterium against various stress conditions, solar radiation, and photo-oxidative stress [25].

In the present study, we employed a green approach for synthesizing nano sized silver particles by using XP as a reducing and stabilizing agent. The rationale behind using XP is that they are well known multifaceted and used as antioxidants and photo-protectants [26]. Based on our knowledge, the present study is the novel report of the synthesis of nano sized silver particles by using the XP under sunlight energy. The pigment and pigment assisted nanomaterial was characterized and were evaluated for its the photo protecting potential of with commercially available sunscreens, antioxidant activity and antimicrobial activity against some Gram positive and negative bacteria.

Materials and methods

Chemicals

Silver nitrate powder ($AgNO_3$) was purchased from sigma-aldrich with 99.99 % purity. Solvents; methanol, ethanol and chloroform were purchased from Sd-fine chemicals (India). All media were purchased from Hi-Media. Two commercial sunscreens with stated sun protection factors (SPFs) of 4 and 10 were purchased from the local store in Jalgaon, India.

Microorganism

The bacteria was isolated from infected plant leaves and primarily identified by morphological and biochemical tests. The further confirmation was carried out by molecular sequencing.

Microbial pigment production

The *Xanthomonas* sp. SVP1 cultivated at 28 °C on selective growth medium plate (Peptone 5 gm/L,Yeast extract 5 gm/L, Glucose 5 gm/L, Calcium carbonate 10 gm/L, Agar 30 gm/L) [27]. The isolated single colony was inoculated in the nutrient medium broth, which were incubated at 28 °C for 24h on shaker. After incubation inoculum was transferred in fresh 100 mL above mentioned liquid medium for pigment production and incubated for 48 h in incubator shaker at 28 °C.

Extraction of pigment

After 48 h incubation the cell pellets were separated by centrifugation at 10,000 rpm for 20 min. The supernatant was decanted and the biomass was washed two times by sterile physiological saline. The

Table 1
Application of bacterial pigment synthesis of silver nanoparticles.

Sr. No.	Pigment	Method	UV visible (nm)	Colour change	Shape	Size (nm)	Reaction type	Application	Reference
1	Actinorhodin	$AgNO_3$ solution of 1 mM mixed with 1mL actinorhodin under sunlight for 15 min	418	Colorless to brown	Irregular	28–50	Sunlight	Antibacterial	[9]
2	Prodigiosin	A mixture of equal volume of culture supernatant and $AgNO_3$ solution was incubated for 60 °C in a water bath until color changed	400–425	Pink to black color	Spherical and ellipsoidal	25.9–34.8	Heated at 60℃	Antibacterial Activity	[10]
3	Monascus pigment	100 μL solution of red pigment in the concentration of 1 mg mL^{-1} was added to 2.5 mL of 2.0 × 10^{-4} M silver nitrate ($AgNO_3$) under direct sunlight	445	Light red colour to dark brown	Spherical shape	10–40	Sunlight	Antibacterial	[11]
4	Carotenoids	A mixture of 1 mL pigment and 5 mL of 1 mM $AgNO_3$ kept overnight at room temperature	420	Light yellow to yellowish brown	–	65	Room temperature	Antioxidants	[12]
5	Flexirubin	A mixture of 10 mL of 1 mM $AgNO_3$ and 1 mL of flexirubin was incubated at room temperature for 30 min	420	Turn brown in colour	Spherical	49	Room temperature	Anticancer	[13]
6	Fucoxanthin	A solution of $AgNO_3$ and Fucoxanthin at a final concentration of 2 mM $AgNO_3$ under light	413	Light yellow to brown	Spherical, polycrystalline spherical	20–25	Presence of light	Antibacterial	[14]
7	Melanin	1mM $AgNO_3$ with 10 mg melanin 100 ml^{-1} 0.1 M KOH at 100 °C for 1h	410	Yellow to dark brown	Spherical	10-50	Heated at 100℃	Antibacterial	[15]
8	C-phycocyanin	A mixture of C-phycocyanin (5 mg/mL) + 10 mL of 1 mM $AgNO_3$ incubated at 25 °C, pH 7, under cool white fluorescent light (50 μM photons m^{-2} s^{-1}) for 48 h	450 and 400	Yellow to dark brown	Spherical	50	Fluorescent light	Monitoring quality of water.	[16]

separated biomass was further subjected for extraction using methanol [28,29]. The mixture was incubated for 2–3 h at 140 rpm under dark condition. Then mixture was centrifuged at 10,000 rpm for 10 min, supernatant was collected and concentrated by vacuum evaporation using Rota evaporator (Buchi Rotavapour). XP was extracted in ethyl ether from above concentrated methanol extract by solvent solvent extraction method. The extracted pigment was dried and stored at −20 °C, and used for further purification, characterization and applications.

Purification and characterization of pigment

The extracted XP was purified by silica gel thin layer chromatography (TLC) technique (GF-254) (Merck, India).The chromatogram was run with solvent system chloroform:methanol (2:1). The presence of XP was confirmed by TLC with slight modification of pervious reported method [30]. The yellow colour band from the TLC plate scrapped and eluted in methanol. After evaporation the pigment was stored at −20 °C. Characterization of XP was carried out with spectroscopic techniques i. e. UV–visible, FT-IR and Mass spectroscopy.

XP mediated synthesis of silver nanoparticles (XP-AgNPs)

The XP mediated synthesis of AgNPs was carried out as follows: 50 μL (1 mg mL^{-1}) of pigment solution was mixed with 950 μL of silver nitrate solution (1 mM $AgNO_3$) (pH-7.0 ± 0.2) in clean, dry glass tubes. The tube was then vigorously shaken to ensure appropriate reactant mixing and kept in high intensity sunlight (between 12.0 and 2.0 pm). The visible colour shift of silver salt in solution was then monitored. Simultaneously, $AgNO_3$ (1 mL $AgNO_3$ without pigment) and pigment (50 μL pigment in 950 μL water) controls were run under the identical conditions [11,31].

Characterization of XP mediated silver nanoparticle (XP–AgNPs)

UV–Vis spectrophotometric analysis

The pigment assisted nanoparticles were analyzed by scanning orange-brown XP–AgNPs solution by UV–Vis spectrophotometer (Shimadzu UV 1800i, Japan) in a range of 200–800 nm.

Field emission scanning electron microscopy (FESEM), High-resolution transmission electron microscopy (HR-TEM), and Selective area electron diffraction (SAED) analysis

A field emission scanning electron microscope (FE-SEM Hitachi S4800, Japan) was used to project the surface structure of XP-AgNPs. High resolution transmission electron microscopy and selected area electron diffraction was used to determine the crystal structure and size of the crystal. The XP–AgNPs solution was sonicated for 10 min and a small volume was loaded on a carbon-coated copper grid. Subsequently, the copper grid was placed under infra-red lamp for 15 min to completely dry the sample. High resolution images of XP-AgNPs were recorded in the bright field using TEM (FEI, USA) operated at 300 kV [11].

Energy dispersive spectroscopy (EDAX) analysis

The presence of elemental silver in synthesized XP-AgNPs solution was estimated by energy dispersive spectroscopy (Brucker, Germany).

Dynamic light scattering (DLS) and Zeta potential analysis

The synthesized nanomaterial was analyzed for it's nanomaterial dispersion by dynamic light scattering and Zeta potential analysis (Malvern Instruments, USA).

X-ray diffraction (XRD)

X-ray diffraction was used to determine the crystallinity of XP-AgNPs (PANalytical Xpert Pro MRD Diffractometer). The spectra was measured in the range of 20 to 80° range at room temperature, with a scanning rate of 0.4°/min. Silver nanoparticles were analyzed using the Debye-Scherrer equation, to determine average grain size as follows [10,32].

$$D = \frac{K\lambda}{\beta\cos\theta}$$

Where 'D' is the crystallite size, 'K' is constant (0.94), λ is the wavelength of the X-ray source (0.15406 nm), β is full width half maximum (FWHM), and θ is the diffraction angle.

Fourier transforms infrared (FT–IR) spectroscopy analysis

The purified powder of XP and XP-AgNPs were subjected to FT-IR spectroscopic analysis. KBr pellets were prepared for XP and XP-AgNPs and analyzed on a PerkinElmer instrument with a scanning range of 450–4000 cm^{-1}.

Antimicrobial assay of XP and XP-AgNPs

The antibacterial activity of XP-AgNPs was assessed by employing the well diffusion method. Four bacterial pathogens were tested as a representative of Gram positive and Gram negative viz; *Bacillus subtilis*, *Staphylococcus aureus*, *Pseudomonas aeruginosa*, and *Escherichia coli*. The bacterial cultures were grown overnight in Luria Bertani (LB) broth; thereafter, 100 μL (10^5 CFU mL^{-1}) of culture was spread uniformly on agar plates, and wells were punctured (6 mm) by using a sterile well borer. Different concentrations of XP-AgNPs, control XP, and standard antibiotic (Ampicillin) were loaded in wells. The inoculated plates were incubated at 37 °C for 24 h. The plates were subjected for determination of antibacterial activity by measuring the zone of inhibition [33].

Determination of sunscreen protection potential of pigment

The *in vitro* spectrophotometric technique was slightly modified to assess the sunscreen protection potential of pigment by measuring sun protection factor (SPF) of commercial sunscreens (SPF 4 and 10) and sunscreens fortified with XP and XP-AgNPs [34–36]. Commercial sunscreens with labeled SPF of 4 and 10 served as the standard control while XP and XP-AgNPs were added to the above mentioned sunscreens at a concentration of 4 % as test. The experimental and control sunscreen formulations (0.1 g) was mixed with 10 mL of ethanol (in triplicate). All samples (both the control and the pigment-supplemented samples) underwent a 5 min ultrasonic treatment before being centrifuged at 10,000 rpm. The solution for measurement was prepared by adding 2.0 mL of ethanol in the 0.5 mL aliquots of supernatant [37].

Optical density of ethanol serving as a blank and the optical densities of test solutions were determined in the UV spectrum between 200 and 600 nm at intervals of 10 nm. According to Mansur et al. (1986), SPFs were computed based on three independent studies using the formula below [38]:

$$\mathrm{SPF} = \mathrm{CF}\,\mathrm{x}\sum_{290}^{320}\mathrm{EE}(\lambda)\times\mathrm{I}(\lambda)\times\mathrm{Abs}(\lambda)$$

Where CF (correction factor) = 10; EE (λ) = erythmogenic effect of radiation with wavelength λ; Abs (λ) = absorbance value of a solution at a wavelength λ; and I (λ) = solar intensity spectrum. EE (λ) × I are the standard tabular values and determined as per Sayre et al. [39].

Antioxidant potential determination by DPPH radical scavenging assay

Radical scavenging activity of XP-AgNPs was determined by DPPH

(1,1-Diphenyl- 2-picrylhydrazyl) assay with a slight modification of previously describe method [35]. In brief, 40 μL of XP and XP-AgNPs (10 mg mL^{-1} in DMSO) was mixed with 2.96 mL DPPH (0.1 mM) solution. The mixture was vigorously shaken and incubated at room temperature for 30 min in dark conditions. L-Ascorbic acid (LAA) was used as a positive control. The absorbance was measured at 517 nm. The scavenging activity rate was calculated using the following formula [40],

$$\%\ \text{Inhibition} = \frac{(\text{Abs Control} - \text{Abs Test})}{\text{Abs Control}} \text{ x } 100$$

Where Abs control is the absorbance of DPPH solution, Abs Test is the DPPH + XP/XP-AgNPs.

Results

Characterization and identification of XP

Xanthomonas sp. (SVP 1) was exploited for pigment production and further the yellow membrane bound pigment was extracted in methanol and purified by TLC. The purified XP show peak at 445 nm in UV–Vis spectroscopy [30,41]. Similarly in FT-IR analysis the frequencies at 3407.64 and 2933.83 cm^{-1} show C—H stretching, 2854.55 cm^{-1} show sp^3 C—H stretching, 1634.69 cm^{-1} show C═C stretching, 1562.94 cm^{-1} show C═C aromatic stretching, 1409.09, 1377.61, 1240.36, and 1044.15 cm^{-1} for C—H bending and C—O (ether) were present in XP [42]. The purified XP *m/z* 478 Dalton was recorded in mass spectroscopy.

Characterization of XP-AgNPs

Various analytical methods were used for the characterization of XP-AgNPs.

Visible observation and UV–vis spectroscopic analysis

A rapid change in color of $AgNO_3$ solution (1 mM) was observed after challenging with XP yellow pigment (50 μL) and succeeding exposure to sunlight (5 min). The XP added to the silver nitrate solution changed the color of silver nitrate from colourless to light yellow which was further changed to dark yellow-orange after incubation under sunlight (Fig. 1a). The development of the yellow-orange color has confirmed the reduction of bulk silver nitrate into nanoparticles. Synthesis of XP-AgNPs was further monitored and confirmed by UV–vis spectroscopic analysis showing the absorption peak at 420 nm (Fig. 1a) due to the surface plasmon resonance phenomenon of AgNPs [28,43].

The effect of substrate ($AgNO_3$) concentration on XP-AgNPs synthesis was evaluated by challenging increased concentration of $AgNO_3$ (0.2 mM to 2 mM) to constant XP (50 μL, 1 mg mL^{-1} concentration). The absorbance at 420 nm was increased by increasing the concentration of $AgNO_3$ up to 1 mM and no further increase up to 2 mM (Fig. 1b). Similarly, the formation of XP-AgNPs was monitored measuring the absorbance at several time intervals with fixed concentrations of $AgNO_3$ (1 mM) and XPs (50 μL, 1 mg mL^{-1}). In the case of time dependent synthesis, the absorbance of XP-AgNPs at 420 nm was increased with the incubation time (Fig. 1c).

The peak of XP- AgNPs at 420 nm was observed within 30 to 60 s at

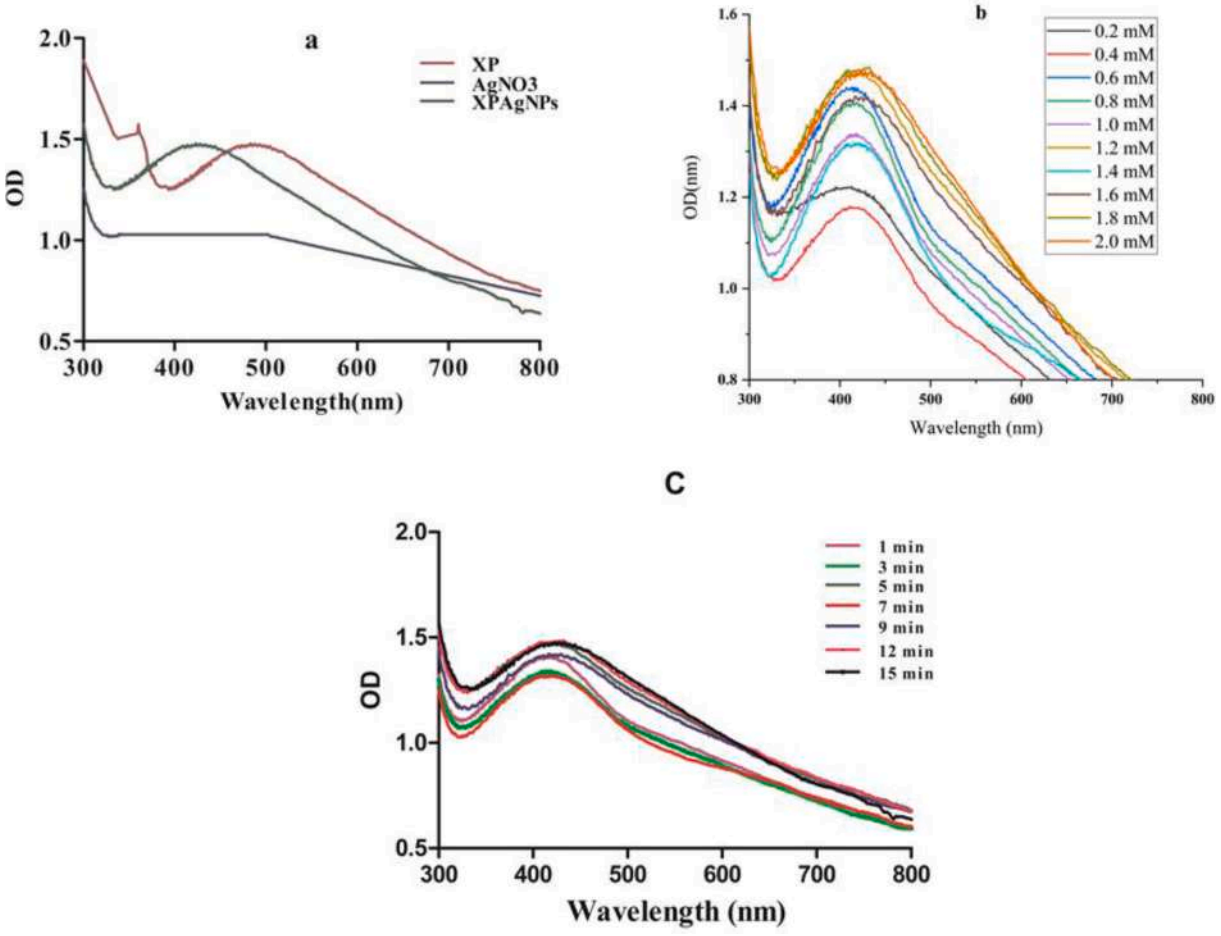

Fig. 1. UV–visible spectrum of Xanthomonadin pigment (XP)-mediated synthesis of silver nanoparticles (XP-AgNPs) (**a**) effect of initial silver salt concentrations (**b**) and incubation time (1 mM $AgNO_3$) on AgNPs synthesis **(c)**

optimized concentration of $AgNO_3$ (1 mM), however, the XP required approximate 10–12 min to complete reduction of $AgNO_3$ into XP-AgNPs (Fig. 1c).

FE-SEM and EDAX analysis

In FE-SEM study, XP-AgNPs were analyzed for their surface topology and morphology. The XP-AgNPs are predominantly spherical and have various irregular shapes (Fig. 2a) instead of single-shape (i.e., spherical, hexagonal, cube, rods) as synthesized by chemical methods. XP-AgNPs size was between 30 and 100 nm (Fig. 2a). Energy dispersive spectroscopy (EDAX) confirmed the presence of elemental silver in XP-AgNPs solution (Fig. 2b).

HR-TEM and SAED analysis

The size, shape, and crystalline nature of the XP-AgNPs were further confirmed by HR-TEM and SAED analysis, respectively. Fig. 3a depicted the well dispersed spherical shape XP-AgNPs with an average size of 58 nm. Similarly, Fig. 3b shows the apparent and unwavering lattice fringes and a diffraction ring with spot patterns in the SAED pattern (inset of Fig. 3b), which confirms the crystalline nature of XP-AgNPs.

DLS and Zeta potential analysis

The distribution of XP-AgNPs in solution was measured by employing dynamic light scattering (DLS). Particle size of XP-AgNPs was in the range between 30 and 100 nm (Fig. 5a). While, the XP-AgNPs show a zeta potential value of −17 mV, indicating fair stability of XP-AgNPs in solution (Fig. 5b).

X-ray diffraction analysis

A technique used to characterize the structure of crystalline material is X-ray diffraction. This technique can be used to analyze crystal lattice parameters, phase, texture, or even stress of samples. In the X-ray diffractogram for the synthesized XP-AgNPs, distinct diffraction peaks were observed at angles 24.57°, 29.88°, 32.17°, 33.06°, 35.76°, 39.34°, 40.34°, 43.75°, 46.45°, 48.02°, 49.34°, 49.99°, 54.06°, and 56.36° indexed (Fig. 4). The calculated value for the XPmediated silver crystallite size was found to be approximately 63.06 nm.

Possible mechanism of XP-AgNPs synthesis by FT-IR analysis

FT-IR analysis was used to elucidate the possible mechanism for reduction of bulk $AgNO_3$ into AgNPs. XP and $AgNO_3$ reacts in methanol, Ag from $AgNO_3$ binds towards the acidic terminal of XP (Fig. 6a). IR spectra of $AgNO_3$ indicated absorption at 1384 cm^{-1} corresponds to significant Ag peak which was retained in XP-Ag complex. The broad absorption at 3444.05 cm^{-1} corresponds to O-Ag bonding from $AgNO_3$. Moreover, as compared to XP the sharp peak at 3407.64 cm^{-1} was observed in XP-Ag complex due to the interrupted hydrogen bonding intervened by AgNPs in acidic functional group. Preferentially the peak in XP at 2929.98 cm^{-1} originated by C═C-H (C—H) stretching was almost vanished in XP-Ag complexation. It was due to the Ag interaction at acidic terminal deviated electron flow from the Ag to acidic C═O complex. The significant absorption at 1637.02 cm^{-1} associated with asymmetric and symmetric stretching properties of the CO_2 carboxylate groups observed both in XP and XP-Ag. Similarly, the peaks at 1121.17 and 1046.23 cm^{-1} were associated with C—O—C stretches of ether confirm -O-CH_3. The sharpness of peaks at 678.78 cm^{-1} and 1637 cm^{-1} in XP decreases in XP-AgNPs may be due the intervening of AgNPs in -O-CH_3 and Br bonded to aromatic ring. The possible mechanisms of XP-AgNPs synthesis was due to the formation of Ag-acid informal bonding which was later reduced to silver nitrate in the nanoform particles. The presence of different redox functional groups and extended heteroatoms with aromatic conjugation in azaphylon-type XP (in the presence of sunlight) has been implicated in the synthesis of AgNPs in ecofriendly (water) systems. FT-IR spectra (XP-AgNPs) show complexation of $AgNO_3$ with acid functional group of XP which was later reduced in presence of sunlight to XP-AgNPs (Fig. 6b).The mechanism of XP nano synthesis was explained here solely based on FT-IR frequencies for reduction of bulk silver into nanoparticles, still it needs to further explored.

Applications of XP-AgNPs

Photo-protective potential of XP-AgNPs

The sunlight protecting mechanism was evaluated by measuring the sun protecting factor of pigment at different concentration and with fortification of standard sunscreen with pigment. The sun protection factor (SPF) was calculated by measuring the absorbance within 290–320 nm [35,44–46]. It was revealed that the two commercial sunscreens with claimed SPF values of 4 and 10 empirically showed SPF

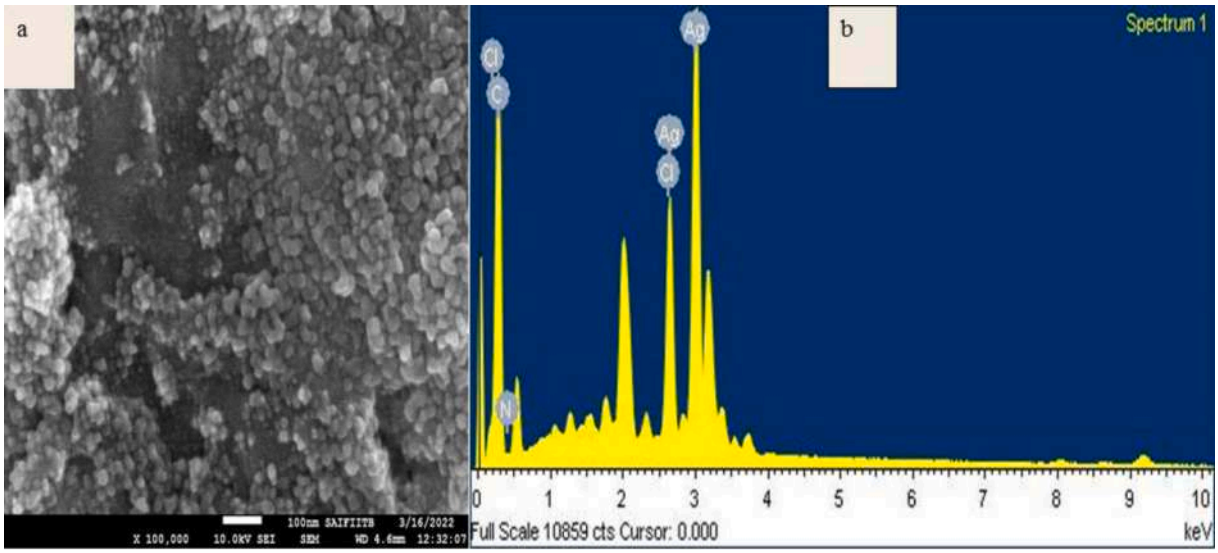

Fig. 2. Field-Emission-Scanning Electron Microscopy of (FE-SEM) **(a)** and EDAX of AgNPs **(b)** synthesized using Xanthomonadin pigment.

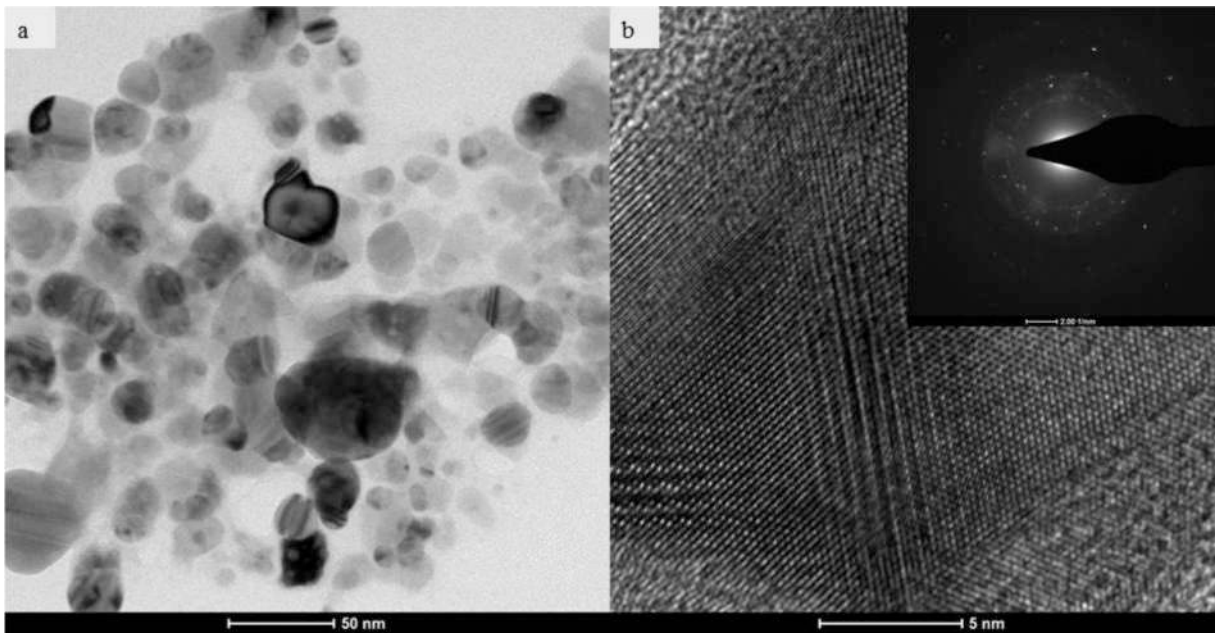

Fig. 3. High-Resolution Transmission Electron Microscopy (HR-TEM) of XP–AgNPs; TEM images of XP–AgNPs **(a)** and HR-TEM images with SAED patterns of XP–AgNPs shows in the inset **(b)**.

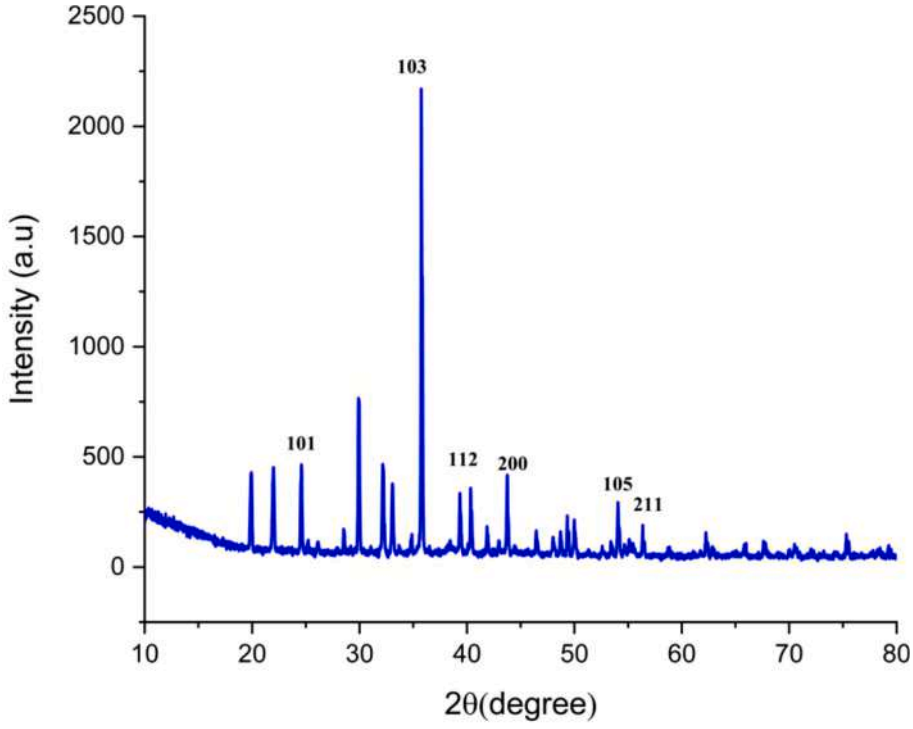

Fig. 4. XRD analysis of XP-AgNPs

values of 4.60 ± 0.011 and 7.41 ± 0.013, respectively.

Commercially available sunscreens having 4 and 10 labeled SPF showed drastic enhancement in SPF value when combined with XP pigment (4 % w/w). Sunscreen (SPF 4.60) and sunscreen SPF (7.41) fortified with pigment had improved SPF (14.87) i.e. 271.75 % enhancement and SPF 18.52 i. e. 85.2 % enhancement respectively (Table 2). The pigment mediated silver nanomaterial fortification in standard sunscreen also showed significant increase in sun protecting factor (Table 2).

DPPH radical scavenging activity

Antioxidants are well known for protecting the skin against free radicals. In the present study, the potential of XP and XP-AgNPs as an antioxidant for protection of skin from free radicals was evaluated by antioxidant assay. Several compounds extracted from Xanthomonas are known to use in cosmetic preparation for their antioxidant and nutri-cosmetic potential [35,45,47]. In the present investigation, DPPH radical scavenging assay was employed to determine the antioxidant potential of XP and XP-AgNPs. As a result, the DPPH assay revealed that

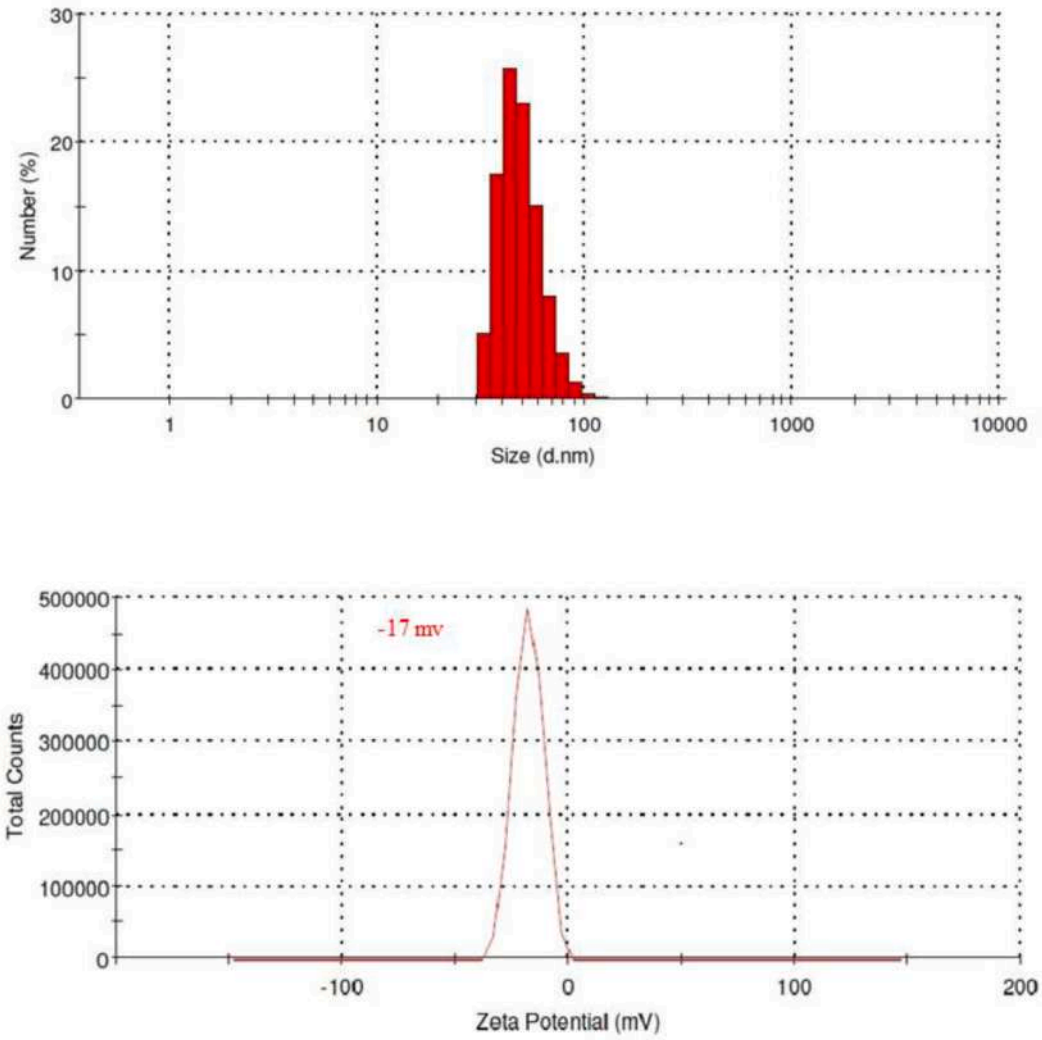

Fig. 5. Particle size analysis **(a)** and zeta potential of XP-AgNPs **(b)**

both XP and XP-AgNPs have substantial radical scavenging activity (Fig. 7). The IC_{50} values for XP, XP-AgNPs, and L-Ascorbic acid, were recorded as 46.21 μg mL^{-1}, 21.62 μg mL^{-1} and 7.44 μg mL^{-1} respectively.

Antimicrobial activity of XP-AgNPs

The yellow colour XP was inactive against the tested bacteria however the XP-AgNPs show excellent antibacterial activity (Table 3 and Fig. S1 supplementary). Among the tested bacteria, susceptibility wise Gram positive bacteria were more susceptible to XP-AgNPs; 13.33 to 16.67 mm zone of inhibition was recorded at 20 μg mL^{-1}concentration. While in Gram negative bacteria particularly for *E. coli*, 60 μg mL^{-1} concentration of XP-AgNPs was required to equivalent the 12.33 mm diameter of zone of inhibition. This organism specific activity of XP-AgNPs is might be due to the outer cell architecture difference between the Gram positive and Gram negative bacteria [35].

Discussion

Green approach for synthesizing nanomaterials is always better than the existing chemical and physical methods. Biological materials, small organisms, and their secondary metabolic products are well known for reducing bulk metal salts into nanosized particles. The protein, carbohydrate, flavonoids, aromatic compounds, cyclic and long chains with free CH, OH, and C—H—C groups are mainly attributed for the synthesis of metal nanoparticles. In the present investigation, we used XP, a yellow color membrane bound pigment extracted from a bacterium *Xanthomonas* sp (SVP1), as a reducing and capping agent for the synthesis and stabilization of silver nanoparticles. Structurally, XP consists of the long polyene moiety with free terminal hydroxyl and carboxyl groups that may be accountable for interacting with bulk silver nitrate, and succeeding exposure to sunlight may result in the reduction of bulk silver nitrate into nanosized particles. Many publications reported a similar mechanism for synthesizing silver and other metal nanoparticles utilizing microbial pigments under the sunlight [48,49]. Microbial pigments consisting of lactone group with carbonyl and hydroxyl group successfully reduced the bulk silver and gold materials into nanoparticles; the opening of the lactone group and formation of carboxylic acid was the mechanism behind the reduction and formation of metal nanoparticles [11,31]. In contrast, in the present study, we did not observe the disappearance or opening of the lactone ring present in the structure of XP. Thus, the free carbonyl and hydroxyl groups present in XP may be responsible for the synthesis of silver nanoparticles; however, further studies merit exploring the mechanism of XP in reducing bulk silver nitrate.

The peculiar characteristics of the XP-AgNPs were thoroughly analyzed. First and foremost, the color of the solution of XP mediated synthesized AgNPs was rapidly turned from colorless to orange-brown and showed a sharp peak at 420 nm in the spectrophotometric

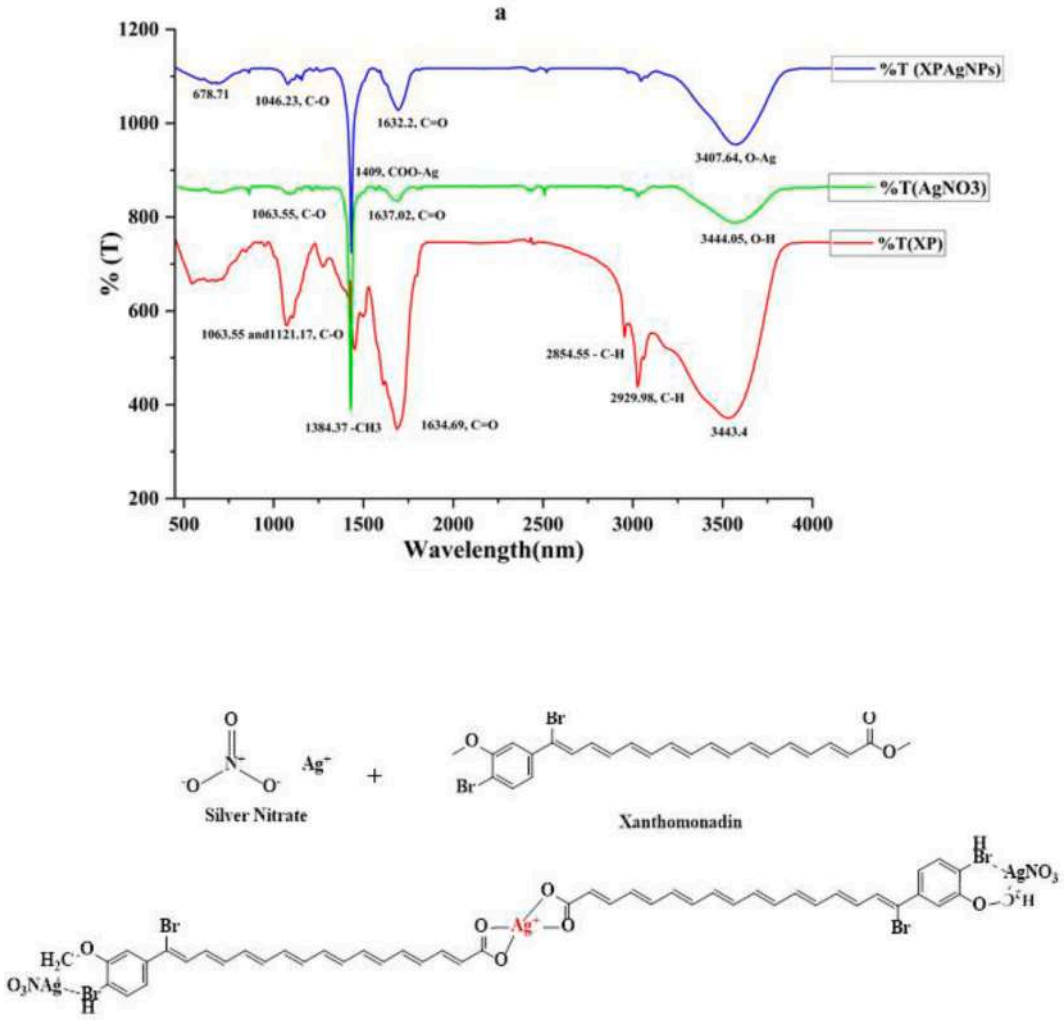

Fig. 6. FT-IR spectrum of XP, $AgNO_3$ and XP–AgNPs **(a)** possible mechanism of interactions of XP with $AgNO_3$ for formation and stability of AgNPs **(b)**.

Table 2
Sunscreen Protection Factors (SPFs) for commercial sunscreen preparations and supplementation with XP

Commercial sunscreen	SPF	Calculated SPF for Sunscreens	SPF XP + Sunscreens	SPF XP-AgNPs + sunscreens
Sunscreen 1	4	4.60 ± 0.011	14.87 ± 0.015	7.32 ± 0.2
Sunscreen 2	10	7.41 ± 0.013	18.52 ± 0.020	11.44 ± 0.4

Note: results are the mean of triplicates.

scanning. This indicated the interaction of XP with $AgNO_3$ and rapid synthesis of XP-AgNPs under sunlight. Similarly, the results of the high resolution microscopy revealed spherical XP-AgNPs with crystalline nature, which is as per previous microbial pigments mediated silver nanoparticles synthesis [32,50]. The XP-AgNPs showed confined particle size distribution and negative zeta-potential values, indicating good stability in solution. The stability of AgNPs might be due to the capping of pigment residues on the surface of XP-AgNPs, which protects them from agglomeration.Various residues of the protein, carbohydrate, and microbial colour pigments were known to act as capping and stabilizing agents for the metal nanoparticles [4].

The genesis of free radicals may occur when the skin is exposed to UV light [35], which is responsible for permanent skin damage. A variety of sunscreens externally applied to the skin, successfully protect it from sunburn. The sunscreen does this through the absorption or repulsion of UV rays (290–320 nm) with the help of different chemical and physical sun protecting molecules added to the sunscreen preparations [35]. Many publications demonstrated the photo-protective potential of XP [26,51]. In light of that, the photoprotection or enhancement of the sun protection factor of commercial sunscreens in the presence of XP and anti-oxidant activity was determined. Chemically the long polyene structure of XP has the potential to absorb the UV–visible light and protect the cell from photodamage. XP may react with different organic molecules present in the commercial sunscreen preparations resulting into more efficient photoprotection. Likewise, the addition of XP-AgNPs increased the SPF of commercial sunscreen as similar to the XP, which may be due to the further contribution of AgNPs in the enhancement of SPF. Our results are in agreement with Borase et al who reported the ability of gold nanoparticles to enhance the SPF of commercial sunscreens [8]. Although the SPF values are appear slightly increase than that pigment but for synthesis of these nanomaterial least amount of pigment was used. For a long time, AgNPs have been well documented for their biocidal activity against various microbial pathogens [52,53]. The present study determined the antibacterial activity of XP-AgNPs against four bacterial pathogens. The XP-AgNPs were found to inhibit the tested bacterial pathogens substantially. The bactericidal activity of XP-AgNPs is mainly driven through the interaction of AgNPs with bacterial membrane, pore formation leads to cell death.

Conclusion

The yellow pigment from *Xanthomonas* sp. was extracted, purified

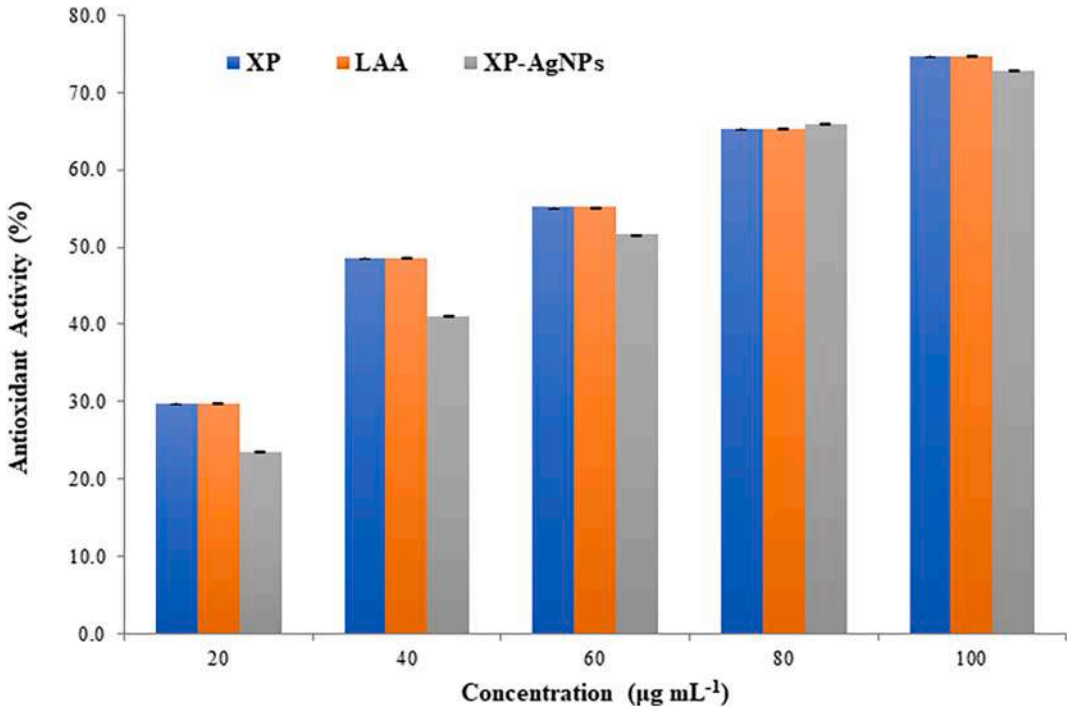

Fig. 7. Antioxidant activity of XP, XP-AgNPs and LAA .

Table 3
Antibacterial activity of XP-AgNPs against bacterial pathogens.

Sr. No.	Test Organism	Zone of Inhibition (mm)				
		20 µg	40 µg	60 µg	80 µg	100 µg
1	*Bacillus subtilis*	13.33 ± 0.5	14.67 ± 0.5	15.67 ± 0.5	17.67 ± 0.5	18.17 ± 0.5
3	*Escherichia coli*	0.00	0.00	12.33 ± 0.5	12.67 ± 0.5	14.33 ± 0.5
2	*Pseudomonas aeruginosa*	15.33 ± 0.5	16.33 ± 0.5	20.67 ± 0.5	23.33 ± 0.5	25.67 ± 0.5
4	*Staphylococcus aureus*	16.67 ± 0.5	18.00 ± 0.5	19.67 ± 0.5	19.33 ± 0.5	21.67 ± 0.5

and characterized by various techniques such as thin layer chromatography, UV visible spectrophotometry, FT-IR and mass spectroscopy as carotenoid pigment i.e. xanthomonadin. The purified pigment was evaluated for its potential of rapid biogenic synthesis of silver nanoparticles. It was observed that in presence of sunlight, pigment reduces silver salt into silver nanomaterial with predominantly spherical shape having size in the range of 30 to 100 nm. This green approach makes this method environment friendly and also help to reduce the burden of pollution in the environment. Pigment was evaluated for its antioxidant potential and found efficient free radical scavenging activity. XP-AgNPs were proved its antimicrobial activity against Gram positive and Gram negative bacteria. The purified pigment also showed its photo-protecting potential through enhancement of SPF factor of commercial sunscreen. The suitability of extracted xanthomonadin and its assisted nanomaterials have the future applicability in various fields like cosmetics and topical antimicrobial preparations. Overall, the xanthomonadin is a versatile natural pigment and its assisted green silver nanoparticles have antioxidant, photo- protecting and biocidal potential.

CRediT authorship contribution statement

Narendra S. Salunkhe: Methodology, Formal analysis, Investigation, Writing – original draft. **Sunil H. Koli:** Writing – review & editing, Software. **Bhavana V. Mohite:** Writing – review & editing, Data curation. **Vikas S. Patil:** Software, Visualization. **Satish V. Patil:** Conceptualization, Supervision, Validation, Writing – review & editing.

Declaration of Competing Interest

The authors declare that they have no known competing financial interests or personal relationships that could have appeared to influence the work reported in this paper.

Acknowledgments

Dr. Satish V. Patil kindly acknowledges and thankful to DST-FIST for providing financial support to the SOLS department, KBCNMU, Jalgaon. Mr. Narendra S. Salunkhe acknowledges and thankful to BARTI for financial support through the fellowship (Fellowship No. BARTI/Fellowship/BANRF-2020/21-22/850).

Appendix A. Supplementary data

Supplementary data to this article can be found online at https://doi.org/10.1016/j.rechem.2022.100663.

References

[1] N. Jain, A. Bhargava, S. Majumdar, J.C. Tarafdar, J. Panwar, Extracellular biosynthesis and characterization of silver nanoparticles using Aspergillus flavus NJP08: a mechanism perspective, Nanoscale 3 (2) (2011) 635–641, https://doi.org/10.1039/c0nr00656d.
[2] Https://statnano.com/nanomaterials, "Nanomaterials Database | STATNANO," *Statnano.Com.* 2022.
[3] S.V. Patil, et al., Phytosynthesized gold nanoparticles- *Bacillus thuringiensis* (Bt – GNP) formulation : a novel photo stable preparation against mosquito larvae, J. Clust. Sci. 29 (4) (2018) 577–583, https://doi.org/10.1007/s10876-018-1368-4.
[4] S.M. Albukhari, M. Ismail, K. Akhtar, E.Y. Danish, Catalytic reduction of nitrophenols and dyes using silver nanoparticles @ cellulose polymer paper for the resolution of waste water treatment challenges, Colloids Surfaces A Physicochem. Eng. Asp. 577 (March) (2019) 548–561, https://doi.org/10.1016/j.colsurfa.2019.05.058.

[5] A. Patel, et al., Integrating biometallurgical recovery of metals with biogenic synthesis of nanoparticles, Chemosphere 263 (2021), https://doi.org/10.1016/j.chemosphere.2020.128306.

[6] A. Chokriwal, M. Sharma, A. Singh, Green nanoparticle synthesis and their applications, *Int. J. Pharmacogn.* 2 (3) (2015) 110–115, https://doi.org/10.13040/IJPSR.0975-8232.IJP.2(3).110-15.

[7] P.P. Gan, S.F.Y. Li, Potential of plant as a biological factory to synthesize gold and silver nanoparticles and their applications, Rev. Environ. Sci. Biotechnol. 11 (2) (2012) 169–206, https://doi.org/10.1007/s11157-012-9278-7.

[8] H.P. Borase, et al., Plant extract: a promising biomatrix for ecofriendly, controlled synthesis of silver nanoparticles, Appl. Biochem. Biotechnol. 173 (1) (2014) 1–29, https://doi.org/10.1007/s12010-014-0831-4.

[9] M.P. Narsing Rao, M. Xiao, W.J. Li, Fungal and bacterial pigments: Secondary metabolites with wide applications, Front. Microbiol. 8 (JUN) (2017) 1–13, https://doi.org/10.3389/fmicb.2017.01113.

[10] D. Karthika, K. Vadakkan, R. Ashwini, A. Shyamala, J. Hemapriya, S. Vijayanand, Prodigiosin mediated biosynthesis of silver nanoparticles (AgNPs) and evaluation of its antibacterial efficacy, Int. J. Curr. Microbiol. App. Sci 4 (11) (2015) 868–874.

[11] S.H. Koli, B.V. Mohite, R.K. Suryawanshi, H.P. Borase, S.V. Patil, Extracellular red Monascus pigment-mediated rapid one-step synthesis of silver nanoparticles and its application in biomedical and environment, Bioprocess Biosyst. Eng. 41 (5) (2018) 715–727, https://doi.org/10.1007/s00449-018-1905-4.

[12] H. Sowani, P. Mohite, S. Damale, M. Kulkarni, S. Zinjarde, Carotenoid stabilized gold and silver nanoparticles derived from the Actinomycete Gordonia amicalis HS-11 as effective free radical scavengers, Enzyme Microb. Technol. 95 (2016) 164–173, https://doi.org/10.1016/j.enzmictec.2016.09.016.

[13] C.K. Venil, et al., Synthesis of flexirubin-mediated silver nanoparticles using Chryseobacterium artocarpi CECT 8497 and investigation of its anticancer activity, Mater. Sci. Eng. C 59 (2016) 228–234, https://doi.org/10.1016/j.msec.2015.10.019.

[14] J. Jena, N. Pradhan, B.P. Dash, P.K. Panda, B.K. Mishra, Pigment mediated biogenic synthesis of silver nanoparticles using diatom Amphora sp. and its antimicrobial activity, J. Saudi Chem. Soc. 19 (6) (2015) 661–666, https://doi.org/10.1016/j.jscs.2014.06.005.

[15] S. Roy, S. Shankar, J.W. Rhim, Melanin-mediated synthesis of silver nanoparticle and its use for the preparation of carrageenan-based antibacterial films, Food Hydrocoll. 88 (2019) 237–246, https://doi.org/10.1016/j.foodhyd.2018.10.013.

[16] A.K. Tomer, T. Rahi, D.K. Neelam, P.K. Dadheech, Cyanobacterial extract-mediated synthesis of silver nanoparticles and their application in ammonia sensing, Int. Microbiol. 22 (1) (2019) 49–58, https://doi.org/10.1007/s10123-018-0026-x.

[17] T.G. Smijs, S. Pavel, Titanium dioxide and zinc oxide nanoparticles in sunscreens: focus on their safety and effectiveness, Nanotechnol. Sci. Appl. 4 (1) (2011) 95–112, https://doi.org/10.2147/nsa.s19419.

[18] S. Yuan, J. Huang, X. Jiang, Y. Huang, X. Zhu, Z. Cai, Environmental fate and toxicity of sunscreen-derived inorganic ultraviolet filters in aquatic environments: a review, *Nanomaterials* 12 (4) (2022), https://doi.org/10.3390/nano12040699.

[19] M.U. Gürbüz, "In situ deposition of silver nanoparticles on polydopamine- coated manganese ferrite nanoparticles: synthesis , characterization , and application to the degradation of organic dye pollutants as an efficient magnetically recyclable nanocatalyst," no. March, pp. 1–10, 2021, 10.1002/aoc.6284.

[20] B. Mahdavi, "Green synthesis of NiONPs using Trigonella subenervis extract and its applications as a highly efficient electrochemical sensor, catalyst , and antibacterial agent," no. March, pp. 1–13, 2021, 10.1002/aoc.6264.

[21] A.L.İ.S. Ertürk, G. Elmaci, M.U.L.V.İ. Gürbüz, "Reductant free green synthesis of magnetically recyclable $MnFe_2O_4$ @ SiO_2-Ag core-shell nanocatalyst for the direct reduction of organic dye pollutants," 45(6) 2021, 10.3906/kim-2108-2.

[22] G. Elmaci, "Microwave assisted green synthesis of Ag/AgO nanocatalyst as an efficient OER catalyst in neutral media," 7(1) 2020 61–65, 10.17350/HJSE190300001.

[23] K.P. Madhwani, Safe development of nanotechnology: a global challenge, Indian J. Occup. Environ. Med. 17 (3) (2013) 87–88, https://doi.org/10.4103/0019-5278.130833.

[24] M.M. Mathews-Roth, T. Wilson, E. Fujimori, N.I. Krinsky, Carotenoid Chromophore length and protection against photosensitization, Photochem. Photobiol. 19 (3) (1974) 217–222, https://doi.org/10.1111/j.1751-1097.1974.tb06501.x.

[25] S.Q. An, et al., Mechanistic insights into host adaptation, virulence and epidemiology of the phytopathogen Xanthomonas, FEMS Microbiol. Rev. 44 (1) (2019) 1–32, https://doi.org/10.1093/femsre/fuz024.

[26] L. Rajagopal, C.S. Sundari, D. Balasubramanian, R.V. Sonti, The bacterial pigment xanthomonadin offers protection against photodamage, FEBS Lett. 415 (2) (1997) 125–128, https://doi.org/10.1016/S0014-5793(97)01109-5.

[27] A.G.A.M.P. Starr, C.L. Jenkins, L.B. Bussey, Microbiology 9 (1977) 1–9, https://doi.org/10.1007/BF00428572.

[28] A.R. Poplawsky, S.C. Urban, W. Chun, Biological role of xanthomonadin pigments in *Xanthomonas campestris* pv. campestris, Appl. Environ. Microbiol. 66 (12) (2000) 5123–5127, https://doi.org/10.1128/AEM.66.12.5123-5127.2000.

[29] A.R. Poplawsky, W. Chun, H. Slater, M.J. Daniels, J.M. Dow, Synthesis of extracellular polysaccharide, extracellular enzymes, and xanthomonadin in Xanthomonas campestris: evidence for the involvement ot two intercellular regulatory signals, Mol. Plant-Microbe Interact. 11 (1) (1998) 68–70, https://doi.org/10.1094/MPMI.1998.11.1.68.

[30] C.L. Jenkins, M.P. Starr, The pigment of *Xanthomonas populi* is a nonbrominated aryl-heptaene belonging to xanthomonadin pigment group 11, Curr. Microbiol. 7 (4) (1982) 195–198, https://doi.org/10.1007/BF01568797.

[31] S.H. Koli, B.V. Mohite, H.P. Borase, Monascus pigments mediated rapid green synthesis and characterization of gold nanoparticles with possible mechanism, J. Clust. Sci. 28 (5) (2017) 2719–2732, https://doi.org/10.1007/s10876-017-1254-5.

[32] S.S. Ravi, L.R. Christena, N. Saisubramanian, S.P. Anthony, Green synthesized silver nanoparticles for selective colorimetric sensing of Hg^{2+} in aqueous solution at wide pH range, Analyst 138 (15) (2013) 4370–4377, https://doi.org/10.1039/c3an00320e.

[33] R.K. Suryawanshi *et al.*, "Antimicrobial activity of prodigiosin is attributable to plasma-membrane damage," 6419(July) 2016 10.1080/14786419.2016.1195380.

[34] W. Chun, J. Cui, A. Poplawsky, Purification, characterization and biological role of a pheromone produced by *Xanthomonas campestris* pv. campestris, Physiol. Mol. Plant Pathol. 51 (1) (1997) 1–14, https://doi.org/10.1006/pmpp.1997.0096.

[35] S.H. Koli, R.K. Suryawanshi, B.V. Mohite, S.V. Patil. Prospective of monascus pigments as an additive to commercial sunscreens. 2019 10.1177/1934578X19894095.

[36] A.R. Poplawsky, W. Chun, *Xanthomonas campestris* pv. campestris requires a functional pigB for epiphytic survival and host infection, Mol. Plant-Microbe Interact. 11 (6) (1998) 466–475, https://doi.org/10.1094/MPMI.1998.11.6.466.

[37] A. Fonseca, N. Rafaela, Determination of sun protection factor by UV-Vis spectrophotometry, Heal. Care Curr. Rev. 1 (1) (2013) 1–4.

[38] R.D. Mansur, J.D.S., Breder, M.N.R., Mansur, M.C.D.A., Azulay, Determination of sun protection factor by spectrophotometry. *An. Bras. Dermatol*, 61 1986 121–124.

[39] R.M. Sayre, P.P. Agin, G.J. LeVee, E. Marlowe, A comparison of in vivo and in vitro testing of Sunscreening formulas, Photochem. Photobiol. 29 (3) (1979) 559–566, https://doi.org/10.1111/j.1751-1097.1979.tb07090.x.

[40] H. Zhang, L. Jiang, S. Ye, Y. Ye, F. Ren, Systematic evaluation of antioxidant capacities of the ethanolic extract of different tissues of jujube (*Ziziphus jujuba* Mill) from China, Food Chem. Toxicol. 48 (6) (2010) 1461–1465, https://doi.org/10.1016/j.fct.2010.03.011.

[41] A.R. Poplawsky, W. Chun, pigB determines a diffusible factor needed for extracellular polysaccharide slime and xanthomonadin production in *Xanthomonas campestris* pv. campestris, J. Bacteriol. 179 (2) (1997) 439–444, https://doi.org/10.1128/jb.179.2.439-444.1997.

[42] A.B.D. Nandiyanto, R. Oktiani, R. Ragadhita, How to read and interpret ftir spectroscope of organic material, *Indones. J. Sci. Technol.* 4 (1) (2019) 97–118, https://doi.org/10.17509/ijost.v4i1.15806.

[43] L. Rajagopal, C.S. Sundari, D. Balasubramanian, R.V. Sonti, "The bacterial pigment xanthomonadin offers protection against photodamage," 415 1997 125–128.

[44] A.N. Anuar, M. Hakim, A. Halim, N.H. Rosman, I. Othman, *Valorisation of Agro-industrial Residues – Volume I : Biological Approaches*, no. February. 2021.

[45] A.J. Thompson, W.M. Hart-Cooper, J. Cunniffe, K. Johnson, W.J. Orts, Safer sunscreens: investigation of naturally derived UV absorbers for potential use in consumer products, ACS Sustain. Chem. Eng. 9 (27) (2021) 9085–9092, https://doi.org/10.1021/acssuschemeng.1c02504.

[46] R. Yakoubi, S. Megateli, T. Hadj Sadok, L. Gali, Photoprotective, antioxidant, anticholinesterase activities and phenolic contents of different Algerian *Mentha pulegium* extracts, Biocatal. Agric. Biotechnol. 34 (March) (2021), 102038, https://doi.org/10.1016/j.bcab.2021.102038.

[47] M. Zarkogianni, N. Nikolaidis, Determination of sun protection factor (SPF) and stability of oil-in-water emulsions containing Greek red saffron (*Crocus Sativus* L.) as a main antisolar agent, *Int. J. Adv. Res. Chem. Sci.* 3 (7) (2016) 1–7, https://doi.org/10.20431/2349-0403.0307001.

[48] A.K. Samanta, *ApplSamanta, A. K. (2018). Application of natural dyes to cotton and jute textiles: Science and technology and environmental issues. In Handbook of Renewable Materials for Coloration and Finishing (Issue September 2018). 10.1002/9781119407*, no. September 2018. 2018.

[49] T. Amnuaikit, P. Boonme, "Formulation and characterization of sunscreen creams with synergistic efficacy on SPF by combination of UV filters," 3(8) 2013 1–5, 10.7324/JAPS.2013.3801.

[50] K.S. Prasad, G. Shruthi, C. Shivamallu, Functionalized silver nano-sensor for colorimetric detection of Hg2+ ions: Facile synthesis and docking studies, Sensors (Switzerland) 18 (8) (2018) 1–8, https://doi.org/10.3390/s18082698.

[51] Y. He, X. Cao, A.R. Poplawsky. "Chemical Structure , Biological Roles , Biosynthesis and Regulation of the Yellow Xanthomonadin Pigments in the Phytopathogenic Genus Xanthomonas," 33(5) 2020 705–714, 10.1094/MPMI-11-19-0326-CR.

[52] A.K. Samanta, Application of natural dyes to cotton and jute textiles: Science and technology and environmental issues, no. September 2018. 2018.

[53] B. Rastegari, et al., The story of research into Curdlan and the bacteria producing it, Appl. Microbiol. Biotechnol. 6 (1) (2016) 1–12, https://doi.org/10.1007/s00792-020-01180-2.